arXiv:1612.05454v1 [cond-mat.supr-con] 16 Dec 2016

# Two components of critical current in $YBa_2Cu_3O_{7-\delta}$ films

A. V. Kuznetsov, I. I. Sanninkov and A. A. Ivanov
*National Research Nuclear University "MEPhI" (Moscow Engineering Physics Institute), Kashirskoe sh. 31, 115409 Moscow, Russia*

Combined action of weak and strong pinning centers on the vortex lattice complicates magnetic behavior of a superconductor since temperature and magnetic field differently affect weak and strong pinning. In this paper we show that contributions of weak and strong pinning into magnetization of the layered superconductor $YBa_2Cu_3O_{7-\delta}$ can be separated and analyzed individually. We performed a careful analysis of temperature behavior of the relaxed superconducting current $J$ in $YBa_2Cu_3O_{7-\delta}$ films which revealed two components of the current $J = J_1 + J_2$. A simple method of separation of the components and their temperature dependence in low magnetic fields are discussed. We found that $J_1$ is produced by weak collective pinning on the oxygen vacancies in $CuO_2$ planes while $J_2$ is caused by strong pinning on the $Y_2O_3$ precipitates. $J_1$ component weakly changes with field and quasi-exponentially decays with temperature, disappearing at $T \simeq 30$–$40$ K. Rapid relaxation of $J_1$ causes formation of the normalized relaxation rate peak at $T \simeq 20$ K. $J_2$ component is suppressed by field as $J_2 \propto B^{-0.54}$ and decays with temperature following to the power law $J_2 \propto (1 - T/T_{dp})^{\alpha}$ where $T_{dp}$ is the depinning temperature. Detailed comparison of the experimental data with pinning theories is presented.

PACS numbers: 74.25.Wx, 74.25.Sv, 74.72.-h, 74.78.-w

## I. INTRODUCTION

Pinning of vortices on defects in type-II superconductors leads to formation of a critical state and appearance of the critical current $J_c$.[1–4] Thermal fluctuations reduce the pinning strength and activate jumps of vortices between pinning centers (defects).[3–6] High temperature superconductors (HTSC) have a small activation energy and a high probability of thermal activation of vortices motion which leads to a giant magnetic flux creep and decay of the superconducting current over time.[3,4,7] As a result the measured current $J$ becomes lower than $J_c$.[7]

For HTSC materials the maximal currents are achieved in a highly textured $YBa_2Cu_3O_{7-\delta}$ films. 2G-tapes with a metal base and the superconducting $YBa_2Cu_3O_{7-\delta}$ layer were developed for high-current applications.[8,9] Great work was done on studying and optimization of the defects landscape in 2G-tapes to obtain high currents in external magnetic fields and at high temperatures, see Ref. 10 for review. As a result, several manufactures produce now long-length tapes with $J$ of several MA/cm$^2$ at liquid nitrogen temperature.[9] Nevertheless the task of improving performance of the tapes by combinations of artificial and natural pinning centers[11] is still actual. Investigations of pinning on natural defects in standard $YBa_2Cu_3O_{7-\delta}$ films play a major role in that work.

There is a large variety of defects in $YBa_2Cu_3O_{7-\delta}$ films such as vacancies, substituting or extra atoms, dislocations, non-superconducting inclusions and so on.[10] The latter two act as *strong* pinning centers. The dislocations[12–14] are induced close to the substrate-film interface and develop up to the film surface.[13] The nano-sized $Y_2O_3$ precipitations[11,15–21] are spontaneously formed during deposition of $YBa_2Cu_3O_{7-\delta}$ films. It was shown that increase of the inclusion density rises the superconducting current[16] while increase of the dislocation density reduces suppression of the current by magnetic field $H$.[12,13]

Point defects, mainly oxygen vacancies in superconducting $CuO_2$ planes, act as *weak* pinning centers. Weak pinning affects magnetic behavior of $YBa_2Cu_3O_{7-\delta}$ films at temperatures below 30–40 K. For example, the exponential dependence $J \propto \exp(-T/T_0)$ was observed in the range $T < 60$ K[9,22–26] while at high temperatures the current decay follows a power law $J \propto [1 - (T/T_c)^n]^{\alpha}$.[20,21,27–30]. Here $\alpha = 1.2$–$2$, $n = 1$ (Refs. 27–30) or 2 (Refs. 20 and 21) and $T_0 \simeq 17$–$32$ K.[9,22–26]

The magnetic flux creep also changes at low temperatures. A peak of the normalized relaxation rate of the current $S = |d \ln J / d \ln t|$ was observed in $YBa_2Cu_3O_{7-\delta}$ films at $T \simeq 20$ K[11,31,32] and the quantum creep was found below 1 K.[7,33–36] The quantum creep and a crossover to two-dimensional superconducting behavior observed at $T < 80$ K[37] revealed an importance of layered structure for superconductivity in $YBa_2Cu_3O_{7-\delta}$.

The analysis of the critical state in HTSC is complicated by presence of weak and strong pinning and the layered structure of HTSC materials. If pinning is weak, the elastic forces of the vortex lattice dominates over the pinning forces.[2–4,38] In this case the concerted action of many weak pins on the elastic vortex lattice is described by the collective pinning theory (CP theory).[3] The collective pinning depends only slightly on parameters of individual pinning centers therefore CP theory is easy to generalize. If pinning is strong, defects acts individually and introduce plastic deformations in the vortex system.[2,3,38] In this case pinning depends on parameters of the defects so many various models were developed for different kinds of defects.[3,5,6,14,27,39,40]

Strong pinning in a layered superconductor, which contains point defects in the superconducting planes and three-dimensional defects in the bulk, was analyzed by

Ovchinnikov and Ivlev[39] (OI theory). They found that the critical current $J_c$ of such superconductor consists of two components produced by in-plane and in-volume pinning. Further developing the OI theory, van der Beek *et al.* considered in-volume pinning and calculated the dependence of $J_c$ on film thickness $d$ and temperature.[19] The dependence $J(d)$ for thin $YBa_2Cu_3O_{7-\delta}$ films was successfully described[19,20] in the frame of extended OI theory[19] by pinning on $Y_2O_3$ inclusions. At the same time the extended theory agree with experimental data on $J(T)$ and $H^*(T)$ only for $T > 30$ K[19,20] since the in-plane pinning was completely ignored by van der Beek *et al.* Here $H^*$ is the crossover field above which $J$ becomes field dependent.

There exists the model describing strong pinning on edge dislocations at low-angle boundaries of crystallites in $YBa_2Cu_3O_{7-\delta}$ films (EDP model).[14,28,41] For some samples this model approximates well the field dependence of the current in a wide range of fields.[14,41,42] At the same time the EDP model is not universal for all $YBa_2Cu_3O_{7-\delta}$ films, some conditions are necessary for its correct application.[42] Restriction of the EDP model may be caused by neglecting of weak pinning which may influence $J(H)$ behavior at low temperatures. $J(T)$ behavior that follows from the EDP model haven't been tested yet.

To clarify the role of weak and strong pinning we performed a careful analysis of temperature behavior of the relaxed superconducting current in different magnetic fields in $YBa_2Cu_3O_{7-\delta}$ films. The analysis allowed us to separate and describe the current components produced by weak and strong pinning.

The paper is organized as follows. Samples and details of $J(T)$ measurements are discussed in Sec. II. Experimental results are presented in Sec. III. At first we show that $J(T)$ behavior observed in our experiments is common for $YBa_2Cu_3O_{7-\delta}$ films. Then analyzing experimental data we separate currents produced by in-plane and in-volume pinning. The separated current components are analyzed in Sec. IV We discuss a relationship between low-temperature peak of the relaxation rate and component of the current produced by weak pinning. Then we show that this component is caused by single-vortex collective pinning in Cu-$O_2$ planes and try to describe it in the frame of CP theory. At the end we consider the component produced by strong pinning and show that is well described by OI theory extended for strong pinning on $Y_2O_3$ inclusions. Our conclusions are presented in Sec. V. The critical current following from OI theory for magnetic field applied along a normal to the superconducting planes is calculated in Appendix.

## II. EXPERIMENTAL DETAILS

Thin epitaxial films of $YBa_2Cu_3O_{7-\delta}$ were prepared by pulsed laser deposition technique using KrF excimer laser. Disk-shaped single crystal plates of $SrTiO_3$ (100) were used as substrates. The deposition took place at substrate temperature about 750° C, the oxidizer pressure ($N_2O$ or $O_2$) varied from 400 to 800 mtorr in different experiments. The velocity filter was used to select the fine part of the ablation plume (atoms and clusters of small size) and obtain better quality of the film surface.[43,44]

The film structure was analyzed by XRD at D8 Discover diffractometer (Bruker) using Cu-$K_\alpha$ radiation. The study confirmed that films were epitaxial and $c$-oriented. No additional phase was detected. The peaks (002), (005) and (007) were used to determine the $c$ lattice parameter and estimate the values of coherent scattering regions and microdeformation. The $c$ lattice parameter was in the range 11.70–11.73 Å, the rocking curve widths $\omega$ of the (005) Bragg peak for best samples was less than 0.2 degree. The oxygen content varied depending on oxidation condition and brought about the variation of $c$-parameter. As follows from the values of the structure parameters presented in Table I, the films had high-quality crystalline structure with small microdeformation and disorientation.

The critical temperatures of the superconducting transition $T_c = 90$–$91$ K were obtained in resistivity measurements performed on witness-samples made in the same deposition process. The samples demonstrated sharp transitions with width of about 1 K. SQUID-magnetometry and study of the magnetic susceptibility in an alternating magnetic field were used to measure temperature of the magnetic transition $T_c^M$. Obtained $T_c$ and $T_c^M$ values are presented in the Table I.

Measurements of a persistent current induced in $YBa_2Cu_3O_{7-\delta}$ film under change of magnetic field were performed using home-built SQUID magnetometer.[45,46] During the measurements a sample was placed inside a copper tube isolated from the LHe bath by a vacuum jacket. Temperature of the sample varied in the range from 4.21 to 300 K via heating of the tube filled with exchange-helium gas. Magnetic field was produced by a NbTi tube enclosed in NbTi solenoid. To apply a field the solenoid was supplied by current and the tube was warmed above $T_c$ by a short heat pulse. After freezing of the field in the tube the current was withdrawn out the solenoid to minimize noises. Magnetic field up to 2100 Oe can be frozen in the tube of 0.3 mm wall thickness. High fields were applied step by step to prevent overheating of the superconducting films by the current induced under the abrupt change of the external magnetic field.[47] At each step the field increment twice exceeded the characteristic field for flux penetration into the film[4,48,49] to make sure that the induced current is high enough to create the critical state throughout the sample. When measurements were performed in zero applied field, a high field was applied at first and the sample was maintained several minutes in this field. Then the field was decreased step by step and at last step the solenoid was warmed together with the tube to remove a magnetic flux frozen in its wire. Due to strong demagnetization effect a self

TABLE I. Parameters of the $YBa_2Cu_3O_{7-\delta}$ thin film samples.[a]

| # | $D$ | $d$ | $c$ | FWHM | $\omega$ | CDB | $\varepsilon_{\rm micro}$ | $T_c$ | $T_c^M$ | $T_{\rm dp}$ | $J$ | $J_1$ | $J_2$ | $D_i$ | $n_i d_{iz}^{9/4}$ | $D_{iz}$ | $n_i$ | $n_i^*$ | $r_d$ | $\langle L\rangle$ |
|---|---|---|---|---|---|---|---|---|---|---|---|---|---|---|---|---|---|---|---|---|
| | mm | nm | Å | degree | | nm | % | K | K | K | $10^6$ | A/cm$^2$ | | nm | $10^{16}$cm$^{-3}$ | nm | $10^{15}$cm$^{-3}$ | | Å | nm |
| Y1 | 2.1 | 550 | 11.707 | 0.096 | 0.112 | 969 | 0.11 | 90 | 88 | 84 | 13.2 | 8.0 | 5.9 | $5\pm1$ | $2.4\pm0.4$ | 3.9 | 4 | 2 | 4.6 | 284 |
| Y2 | 1.8 | 300 | 11.697 | 0.129 | 0.198 | 206 | 0.10 | 90 | 89 | 88 | 10.4 | 3.8 | 7.2 | $14\pm2$ | $0.7\pm0.2$ | 1.8 | 7 | 0.4 | 4.3 | 37 |
| Y3 | 1.8 | 280 | 11.713 | 0.299 | 0.601 | 96 | 0.23 | 90.5 | 89.5 | 82 | 9.1 | 1.2 | 8.3 | $14\pm2$ | $1.1\pm0.3$ | 1.8 | 11 | 0.7 | 5.3 | 46 |
| Y4 | 2.0 | 380 | 11.725 | 0.277 | 0.729 | 150 | 0.26 | 91 | 89 | 75 | 12.8 | 8.3 | 5.2 | $1.8\pm1$ | $80\pm40$ | 14 | 7 | 790 | 4.6 | — |

[a] The (002), (005) and (007) Bragg peaks were used to obtain the lattice parameter $c$, size of the coherent scattering regions (CDB) and the microdeformation $\varepsilon_{\rm micro}$.
The full width on half maximum (FWHM) and the rocking curve width $\omega$ were measured for the (005) Bragg peak.
$T_{\rm dp}$ and $J$ was measured in field $H = 910$ Oe for samples Y1–Y3 and 1530 Oe for sample Y4.
$J$ was taken at $T = 4.21$ K. $J_1$ and $J_2$ are presented for zero temperature.
$D_{iz}$, $n_i$ and $n_i^*$ were calculated for $D_i$ and $n_i d_{iz}^{9/4} = n_i (D_{iz}/\xi_0)^{9/4}$ obtained via fit of experimental curves.
$\langle L\rangle$ was calculated for $B = 910$ G.

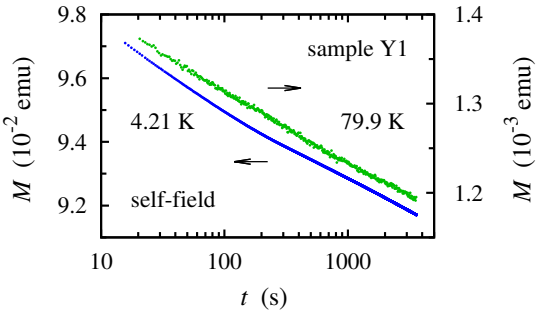


FIG. 1. (Color online) Relaxation curves of remanent moment measured for sample Y1 at low and high temperatures. The moment decays by about 5% and 14% in time-window of the relaxation measurements.

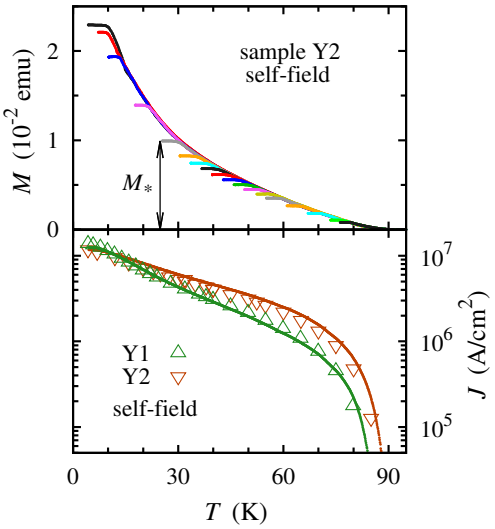


FIG. 2. (Color online) *Top:* Temperature dependences of remanent moment measured for sample Y2 after relaxation for 1 hour. Amplitude of the residual moment $M_*$ obtained for $T = 24.8$ K is shown by arrow. *Bottom:* $J(T)$ dependences obtained from the relaxed moments $M_*$ (triangles) and measured under warming of films during temperature sweep (continuous curves).

demagnetizing field is produced by current flowing in a superconducting film when field is applied perpendicular to the film plane.[50–52] In the critical state this self field exists even after complete removal of external field. The measurements were performed for applied fields of 910 and 1530 Oe and in self-field after removing field of 2090 Oe. These fields were enough to form the homogeneous critical state in samples at all temperatures.

A method of SQUID magnetometry with motionless sample[46,53–56] was used in our experiments. The measurements were performed as follows. The film locked in one of pick-up coils of a superconducting flux transformer was warmed above $T_c$ and cooled in zero field to a desired temperature (ZFC procedure). After that a magnetic field was applied perpendicular to the film plane and a signal caused by change of film magnetic moment with time $\delta M(t)$ due to relaxation was measured for one hour. Then magnetometer indications were reset and the sample was warmed above $T_c$ in order to record its residual moment $M_*$. Combining $M_*$ with data on $\delta M(t)$ we precisely obtained the time dependence of the magnetic moment $M(t)$.[52,57] Examples of $M(t)$ curves obtained at low and high temperatures are shown in Figure 1. As seen, the noise of the curves is considerably lower than the change of the moment due to relaxation.

Preliminary results of the relaxation experiments were published elsewhere.[52,57,58] In the present work we analyze the current obtained from the $M_*(T)$ dependences so let us consider this issue in detail.

The sample was heated at the rate of 5 K/min up to $T = 95$ K during warming and a signal produced by the magnetometer background and the film moment was recorded in steps of 0.1 K. The background signal measured without sample was subtracted from the total one to separate the signal produced by the film only. Inaccuracy of obtaining the film magnetic moment $M$ due to the subtraction did not exceed 0.5% at $T \simeq 80$ K and was considerably smaller at low temperatures. $M(T)$ depen-

dences obtained in such a manner are shown in top Fig. 2. $M(T)$ curves begin with a plateau caused by preceding relaxation of the moment. $M$ values at the plateaus are equal to the residual moments $M_*(T)$.

In bottom Fig. 2 we also presented temperature dependences of the current density calculated as[4,48,49] $J = 24Mc/(\pi D^3 d)$ where $c$ is the light velocity, $D$ and $d$ are the film's diameter and thickness. Two types of $J(T)$ curves are shown for comparison. The first type, obtained from the $M_*(T)$ values, corresponds to a long-time relaxed current. The second one, recorded under film warming immediately after magnetic field removal, presents a short-time relaxed current. As seen in the bottom Fig. 2, shapes of the short- and long-time relaxed curves slightly differ each other. At some temperatures the long-time relaxed current for sample Y1 is greater than the short-time relaxed one while it obviously should be smaller. This artifact is caused by fast temperature sweep during $M(T)$ recording.[59] Since temperature measurement error can affect the $J(T)$ dependences recorded under film warming they are presented below mainly as illustrations. At the same time the $J(T)$ curves obtained from the residual moments correspond to equilibrium temperatures at which the sample was kept more than hour. These temperatures were stabilized and measured with accuracy better than 0.05 K

## III. RESULTS

We start from comparison of measured $J(T)$ dependences with published data to clarify which features of $J(T)$ behavior are common for $YBa_2Cu_3O_{7-\delta}$ films. However the current $J$ itself should be elucidated first. The critical current $J_c$ determined by pinning theories cannot be measured directly because of huge Joule heat dissipated in $YBa_2Cu_3O_{7-\delta}$ films.[60] Therefore either a current $J_T$ measured in transport experiments or a current induced by applied magnetic field are used to characterize the superconducting current. $J_T$ is maintained during measurement by a current source so it does not relax. On the contrary the persistent current $J$ is affected by creep, therefore it is lower than $J_T$.[61] Moreover, dependences of $J$ and $J_T$ on $T$ and $H$ can differ especially at high temperatures and fields. Therefore only data on the persistent current measured in self-field[9,20–30,62] were chosen for verification.[63]

Representative $J(T)$ curves measured for our samples are shown in Fig. 3 in different scales to display $J$ behavior in different temperature ranges. To illustrate a field influence, the curves obtained in self and external field of 910 Oe are shown for sample Y1.

A power law $J_c \propto (1 - T/T_c)^\alpha$ is expected for pinning of vortices on boundaries between crystallites in the films.[27,40] Three temperature ranges with different $\alpha$ values were found for $YBa_2Cu_3O_{7-\delta}$ films.[27–30] The powers $\alpha \simeq 1.2$–2, 0.9–1.2 and 1.4–2.5 were obtained respectively at high[27,28] $T \gtrsim 77$ K, elevated[29,30] 36 K $\lesssim T \lesssim$ 72 K and lower[29,30] 12 K $\lesssim T \lesssim$ 35 K temperatures. As shown in Fig. 3(a), our results well agree with the published data. Fitting curves for sample Y2 demonstrate good approximation by the power law with $\alpha = 1.55$, 1.2 and 2.2 in the above mentioned ranges. Relaxation slightly affects $J(T)$ at low and elevated temperatures and increases the power at high $T$. External field smoothes $J(T)$ and rises the powers in all ranges. Summing up we conclude that our results are consistent with published data.

Since pinning parameters depend on the penetration depth $\lambda(T) = \lambda_0/\sqrt{1-(T/T_c)^4} = \lambda_0/\sqrt{\tau_+\tau_-}$ and the coherence length $\xi(T) = \xi_0\sqrt{(1+(T/T_c)^2)/(1-(T/T_c)^2)} = \xi_0\sqrt{\tau_+/\tau_-}$ of the superconductor[3] one can assume that their temperature change determine $J(T)$ behavior. Here we denoted $\tau_+ = 1 + (T/T_c)^2$, $\tau_- = 1 - (T/T_c)^2$ and $\lambda_0 = \lambda(0)$, $\xi_0 = \xi(0)$. In the frame of CP model[3] Griessen *et al.* obtained that $J_c \propto \tau_-^{7/6}\tau_+^{5/6}$ for $\delta T_c$ pinning and $J_c \propto \tau_-^{5/2}\tau_+^{-1/2}$ for $\delta\ell$ pinning.[65,66] Similar expressions were calculated by Klaassen *et al.* for strong pinning on inclusions of large, $J_c \propto \tau_-^{3/2}\tau_+^{1/2}$, and small, $J_c \propto \tau_-^{5/2}\tau_+^{-1/2}$, size.[64]

The dependence $J \propto \tau_-^\alpha$ with $\alpha = 1.2$–1.4 in self-field at $T \gtrsim 50$ K was observed experimentally in $YBa_2Cu_3O_{7-\delta}$ films.[20] In field of 100 Oe for $T \gtrsim 40$ K the power $\alpha = 1.53$ was found while at high temperatures $T \gtrsim 83$ K a more rapid decay of $J$ was observed.[21] Our results presented in Fig. 3(b) are consistent with the published data. For example, for sample Y2 in self-field for $T \gtrsim 40$ K we obtained $\alpha = 1.52$. The range in which a rapid decay of $J$ is observed shifts to lower temperatures in external field. Thus we conclude again that our results well agree with published data.

The exponential decay $J \propto \exp(-T/T_0)$ was observed at $T <$ 50–60 K in HTSC single crystals,[67–70] $YBa_2Cu_3O_{7-\delta}$ films[22,23,62] and 2G-tapes.[9] Such behavior was attributed to oxygen vacancies acting as weak pinning centers. The scaling temperature depends on field, for example $T_0 = 25$–32 K in self-field[9,23] and $T_0 = 17$–25 K in $H = 1$–200 kOe.[9,23,62] Both increase[9] and decrease[9,23] of $T_0$ was observed in lower fields. As shown in Fig. 3(c), our results are in good agreement again with published temperatures. In the range $T < 60$ K we obtained $T_0 = 33$, 23.5 K for self-field and 17 K for $H = 910$ Oe.

Studying magnetization of solidified $YBa_2Cu_3O_{7-\delta}$-$Y_2BaCuO_5$ composites Martínez *et al.*[70] in the range 40 K $\leqslant T \leqslant$ 80 K found the dependence $J \propto \exp[-3(T/T^*)^2]$ caused by strong pinning on nonsuperconducting $Y_2BaCuO_5$ precipitates. Here $T^*$ is a characteristic temperature. Authors also concluded that at low temperatures both weak and strong pinning centers were effective.[70] Following this conclusion Plain *et al.*[71] proposed the approximation

$$J = J_w \exp(-T/T_w) + J_s \exp\left[-3(T/T_s)^2\right] \qquad (1)$$

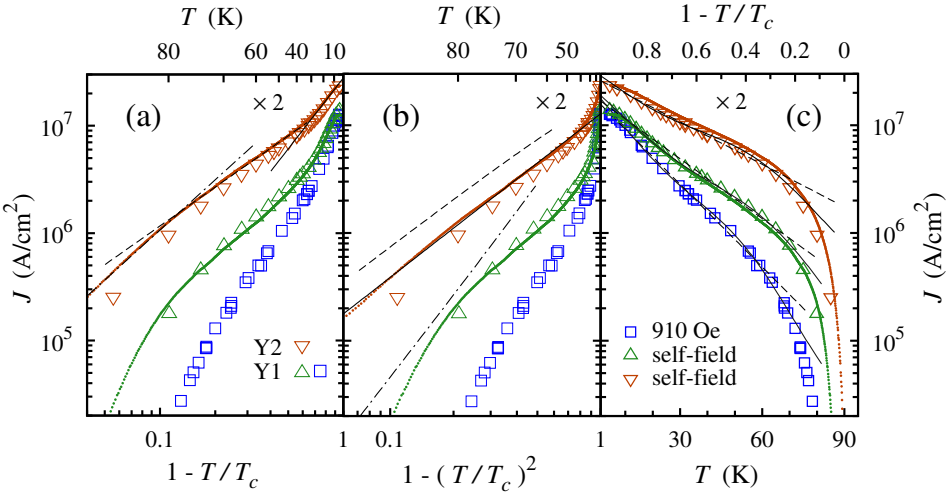


FIG. 3. (Color online) Temperature dependences of the current density of $YBa_2Cu_3O_{7-\delta}$ films in different scales. The curves for sample Y2 are shifted (multiplied by factor 2) to avoid a crossing with ones for sample Y1. *Symbols:* $J(T)$ obtained after relaxation for 1 hour in self-field (triangles) and in field of 910 Oe (squares). Curves with small dots were measured in self-field under warming the samples at sweep rate of 5 K/min. *Panel a:* The lines are approximations $J \propto (1 - T/T_c)^{\alpha}$ with $\alpha = 2.2$ (solid), 1.2 (dashed) and 1.55 (dash-dotted). *Panel b:* Solid line is an approximation $J \propto \tau_-^{\alpha}$ with $\alpha = 1.52$. Dashed and dash-dotted lines are calculated for strong pinning on large $J_c \propto \tau_-^{3/2}\tau_+^{1/2}$ and small $J_c \propto \tau_-^{5/2}\tau_+^{-1/2}$ defects.[64] *Panel c:* Dashed lines are fits by $J \propto e^{-T/T_0}$ with $T_0 = 33$, 23.5 K for Y2, Y1 in self-field and $T_0 = 17$ K for $H = 910$ Oe. Solid lines are fits by the dependence (2): $T_w = 18$, 24 K for Y1, Y2 and $T_s = 52$ K for both samples in self-field; $T_w = 14$ K and $T_s = 43$ K for $H = 910$ Oe.

for the current in $YBa_2Cu_3O_{7-\delta}$ films. Here $w$ and $s$ mark the current components produced by weak and strong pinning. This expression extends the range of the exponential approximation for $J(T)$ to $T \lesssim 75$ K. The temperatures $T_w = 8$–13 K, $T_s = 78$–93 K were found for $YBa_2Cu_3O_{7-\delta}$ films.[24–26]

The dependence $J_c \propto \exp[-3(T/T^*)^2]$ was calculated in theory of strong pinning on columnar pins (*line* correlated disorder).[6] We found that the current $J_c \propto (T/T^*)^2 \exp\left[-(T/T^*)^3\right]$, calculated for compact pins (*point* correlated disorder),[5] gives a better approximation for standard $YBa_2Cu_3O_{7-\delta}$ films. As shown in Fig. 3(c), in the range $T \lesssim 75$ K the $J(T)$ curves are well fitted by the dependence

$$J_c = J_w \exp(-T/T_w) + J_s \left(\frac{T}{T_s}\right)^2 \exp\left[-(T/T_s)^3\right]. \quad (2)$$

We obtained $T_w = 18$ and 24 K and $T_s = 52$ K in self-field. Approximation of the curves by Eq. (1) gave lower $T_w = 8$–10 K and higher $T_s = 85$–93 K values which excellently agree again with published data.

The above analysis confirms validity of all proposed earlier approximations for $J(T)$ for our samples in restricted temperature ranges. The common features of this behavior are a slow quasi exponential decay at low temperatures and a more rapid power-law decay at high ones. We assumed that at least two components are needed to describe $J(T)$ in the whole temperature range. Thermal fluctuations must also be taken into account at high temperatures since they reduce the effective pinning strength and lead to depinning of vortices at some temperature $T_{dp}$ which is less than $T_c$.[3,72] Above the depinning temperature $T_{dp}$ the critical state is destroyed, the persistent current disappears and its relaxation rate becomes zero. We supposed that in vicinity of $T_{dp}$ the current depends on difference $(T_{dp} - T)$ or its powers and found the depinning temperatures for our samples to check this point.

The relaxation rate $R \equiv |dJ/d\ln t|$ for our films is presented in Fig. 4. $R(T)$ curves demonstrate a well-known maximum at low temperatures[7] behind which they smoothly decrease down to zero. We found that above 30 K the rate is well fitted by the dependence $R = \Re \ln^{\beta}(T_{dp}/T)$. To obtain the fitting parameters $\Re$, $T_{dp}$ and $\beta$ we plotted $R$ *vs* $\ln(T_{dp}/T)$ in logarithmic scales and varied $T_{dp}$ to straighten the curves as shown in insets of Fig. 4. Then $\Re$ and $\beta$ were got as shifts and inclination factors of the fitting lines. Obtained values of $T_{dp}$ and $\beta$ slightly depend on magnetic field. For sample Y1 we found $T_{dp} = 84.5 \pm 0.5$ K, $\beta = 1.2 \pm 0.1$ in self-field and $T_{dp} = 84 \pm 0.5$ K, $\beta = 1.4 \pm 0.1$ for $H = 910$ and 1530 Oe. For sample Y2 the same $T_{dp} = 88 \pm 0.5$ K and $\beta = 1.0 \pm 0.05$ were found for all fields. The obtained depinning temperatures are presented in Table I. While the critical temperatures are of the same order for all samples, their $T_{dp}$ strongly differ. For example, $T_{dp} \simeq T_c^M$ for sample Y2 but $T_c^M - T_{dp} \simeq 14$ K for Y4. To be sure in $T_{dp}$ evaluation we checked their maximal and minimal values by direct measurements of the magnetization thermal hysteresis.[72]

$M(T)$ curves measured in field of 910 Oe for samples Y4 and Y2 are presented in Fig. 5. The data were ob-

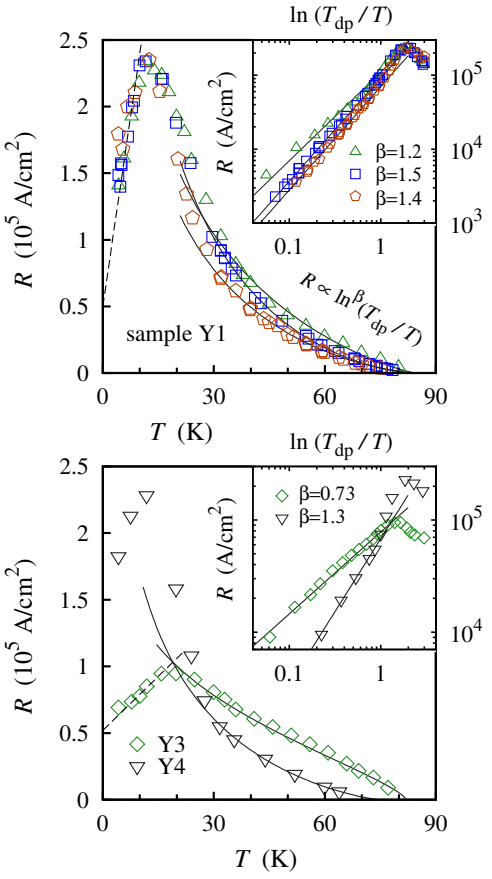


FIG. 4. (Color online) $|dJ/d\ln t|$ *vs* $T$ for $YBa_2Cu_3O_{7-\delta}$ films obtained after relaxation for 1 hour in fields of 1530 Oe (pentagons and triangles down), 910 Oe (squares and diamonds) and in self-field (triangles). The dashed lines extrapolate $R$ to zero temperature. The continuous lines are fits $R = \Re \ln^{\beta}(T_{dp}/T)$. *Inset:* $R$ *vs* $\ln(T_{dp}/T)$ in logarithmic scales. See text for details.

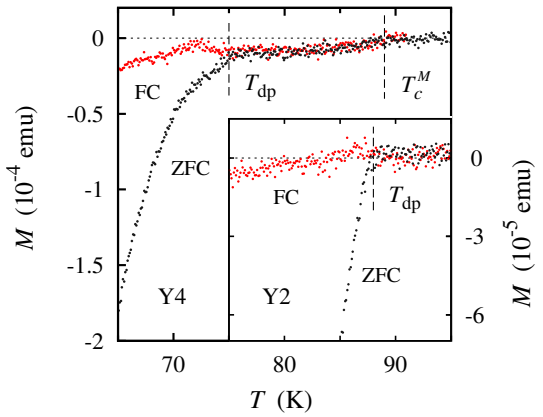


FIG. 5. (Color online) $M(T)$ measured in field of 910 Oe under warming (ZFC) and cooling (FC) of samples Y4 and Y2 (inset). Dashed lines mark depinning and critical temperatures. To avoid a faulty hysteresis[59] the low sweep rate of 3 K/min was used in measurements.

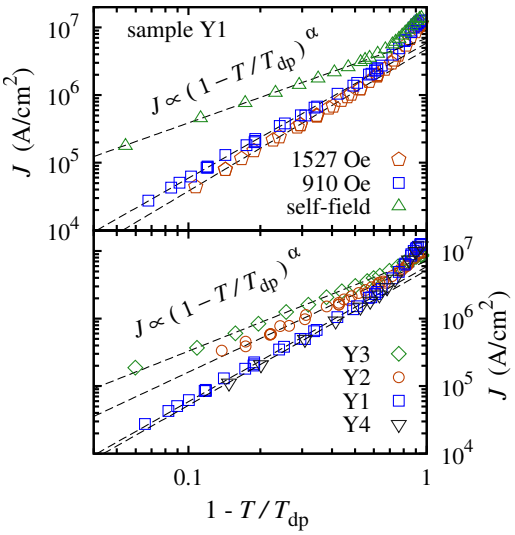


FIG. 6. (Color online) $J$ *vs* $1 - T/T_{dp}$ for $YBa_2Cu_3O_{7-\delta}$ films. Dashed lines are fits by Eq. (3). The curves in bottom panel were measured in field of 910 Oe for samples Y1–Y3 and 1530 Oe for Y4. See Fig. 7, 8 for $\alpha$ and $T_{dp}$ values.

tained after ZFC procedure under warming and subsequent cooling of samples in field of 910 Oe. A thermal hysteresis caused by pinning of vortices is observed below the depinning temperature in Fig. 5. A reversible magnetization is distinctly seen above $T_{dp}$ up to the critical temperature $T_c^M$ for sample Y4 while for Y2 it is indiscernible because of small difference between $T_{dp}$ and $T_c^M$. The measured depinning temperatures coincide with $T_{dp}$ obtained by fit of $R(T)$ dependences.

Taking obtained $T_{dp}$ we found that at high temperatures the current density follows the power law

$$J_2 = J_2(0)(1 - T/T_{dp})^{\alpha}, \qquad (3)$$

therefore we plotted $J$ *vs* $1 - T/T_{dp}$ in logarithmic scales and additionally fit $T_{dp}$ as it was done for the relaxation rate. $T_{dp}$ obtained by $R(T)$ and $J(T)$ fits mostly coincided or differed in the error range of 0.5 K.

$J$ *vs* $1 - T/T_{dp}$ dependences are shown in Fig. 6 in logarithmic scales. The curves demonstrate a pronounced linear part at high temperatures. Top panel of Fig. 6 shows that the curve obtained in self-field differs from ones measured in external fields which are quite similar. The curves obtained in fields of 910 and 1530 Oe for sample Y1 are approximated by the same $T_{dp} = 84$ K, difference of $\alpha \simeq 2 \pm 0.1$ is within the error and only $J_2(0)$ values differ by 19% (see Fig. 7). In the self-field the current demonstrates a weaker temperature dependence with $\alpha = 1.3 \pm 0.1$ and slightly higher $T_{dp} = 84.5$ K.

Analyzing $J(T)$ obtained for different samples we found that $T_{dp}$ and $\alpha$ values do not correlate with each other, at the same time the higher current densities $J_2(0)$ correspond to the lower powers $\alpha$ (see Fig. 8). It can be seen in bottom panel of Fig. 6 where the curves measured in external field are presented for all samples. For exam-

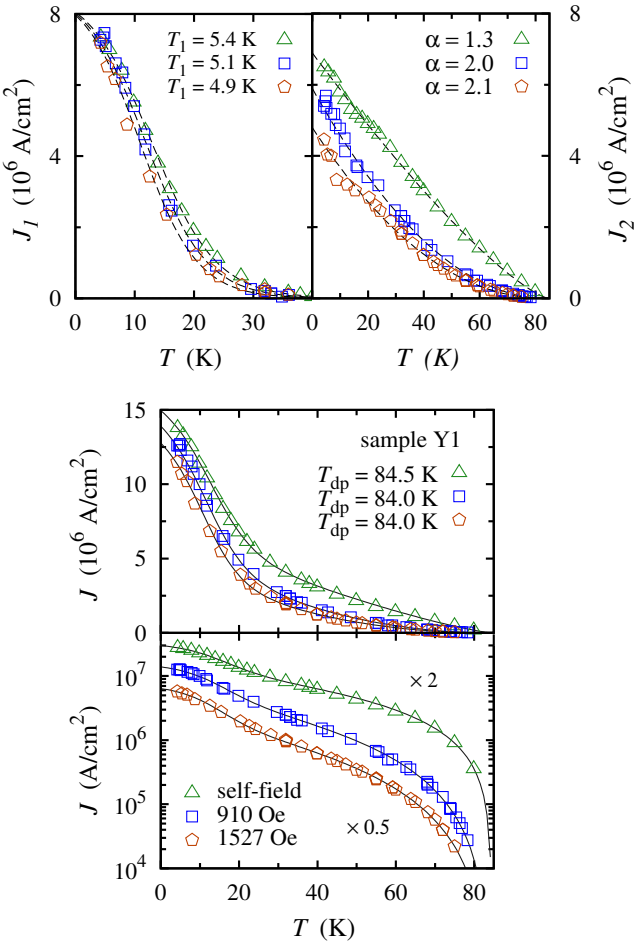


FIG. 7. (Color online) Temperature dependences of the current density of the $YBa_2Cu_3O_{7-\delta}$ film (sample Y1) in different magnetic fields. *Top:* current components $J_1 = J - J_2$ (left) and $J_2 = J - J_1$ (right). Dashed lines are fits by dependences (3) and (4). *Bottom:* Curves $J(T)$ are shown in standard and semilogarithmic scales in order to bring out both low and high temperature behavior of $J$. The curves are shifted (multiplied by shown factors) to avoid a crowding. Continuous lines are sums of fitting curves presented in top panels.

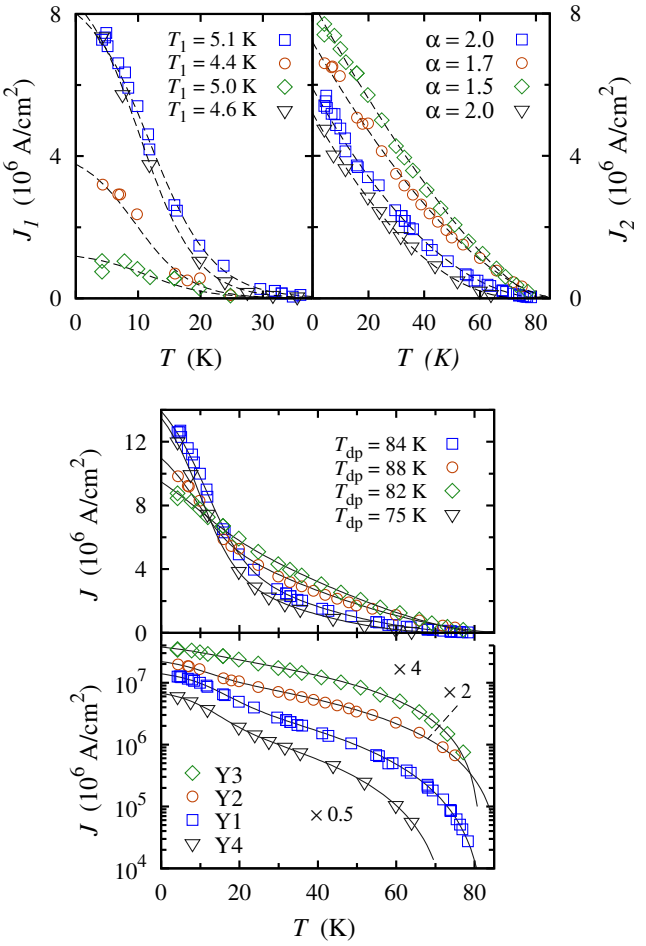


FIG. 8. (Color online) Temperature dependences of the current density of $YBa_2Cu_3O_{7-\delta}$ films in magnetic field of 910 Oe for samples Y1-Y3 and 1530 Oe for Y4. *Top:* current components $J_1 = J - J_2$ (left) and $J_2 = J - J_1$ (right). Dashed lines are fits by dependences (3) and (4). *Bottom:* Curves $J(T)$ are shown in standard and semilogarithmic scales in order to bring out both low and high temperature behavior of $J$. The curves are shifted (multiplied by shown factors) to avoid a crossing. Continuous lines are sums of fitting curves presented in top panels.

ple, for samples Y1 and Y4 the fitting lines demonstrate the same inclination $\alpha = 2.0 \pm 0.1$, but $T_{dp}$ differ by 9 K (see Table I and Fig. 8).

Below 30 K the measured current deviates from the power law (3). Following to Ovchinnikov and Ivlev[39] we supposed that the current consists of two components and subtracted the dependence (3) from the experimental data to analyze a low-temperature behavior. Results of subtraction are shown in left top panels of Figures 7 and 8. As seen, the current $J_1 = J - J_2$ strongly changes in the range $T \lesssim 30$ K. At low temperatures $J_1(T)$ dependence moderates and above 20 K the current gradually falls down to zero at $T \sim 40$ K. We found that low-temperature component of the current can be approximated by an empiric dependence

$$J_1 = \frac{J_1^*}{1 + \exp(T/T_1)/2T_1}, \qquad (4)$$

where the parameter $T_1$ is in Kelvins in the exponent power and dimensionless in its divisor. As seen in Figures 7 and 8 the exponential law (4) well fits $J_1(T)$ dependences. In low field the parameter $J_1^*$ is field-independent and $T_1$ slightly decreases with $H$ (see left top panel in Fig. 7).

The current component $J_2 = J - J_1$ is also plotted for comparison in right top panels of Figures 7 and 8. The ratio of the components $J_1$ and $J_2$ is sample dependent and changes with temperature. For example, $J_2 > J_1$ at all temperatures for samples Y2 and Y3 while $J_1$ becomes more than $J_2$ for Y1 and Y4 at low temperatures. The

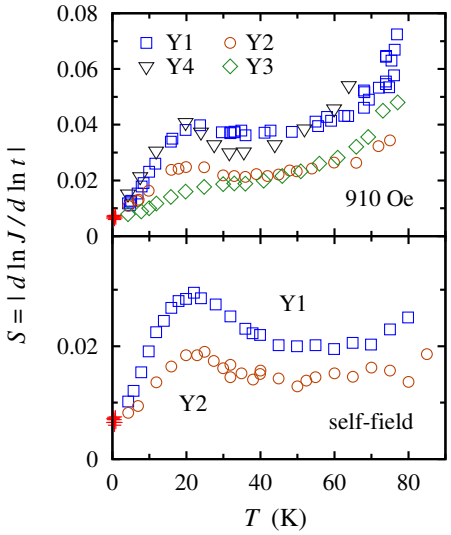


FIG. 9. (Color online) $|d\ln J/d\ln t|$ *vs* $T$ for $YBa_2Cu_3O_{7-\delta}$ films obtained after relaxation during 1 hour in field of 910 Oe (1530 Oe for sample Y4). Crosses are data by Fruchter *et al.*[33] obtained in the range 0.09 K $\leq T \leq$ 0.9 K at $H = 2$ kOe.

ratio determines temperature behavior of total current. Though $J$ is higher in samples Y2 and Y3 at elevated temperatures, at $T \lesssim 15$ K it becomes higher in Y1 and Y4 because of rapid increase of large $J_1$ component.

$J(T)$ curves and sum of $J_1(T)$ and $J_2(T)$ fits are presented in bottom panels of Figures 7 and 8. As seen, the current change by about three orders of magnitude is well approximated. Thus analysis of the separated current components allows us empirically describe $J(T)$ at all temperatures.

## IV. DISCUSSION

Let us consider a relation between the components and relaxation of the current. Comparison of the relaxation rates $R(T)$ with $J_1$ components in Figs. 4 and 8 demonstrates a correlation: the larger $J_1$ the larger $R(T)$ maxima. $J_1$ rapidly decays with both time and temperature therefore it is evidently produced by weak pinning on point defects having a small pinning energy.

The normalized relaxation rate $S \equiv R/J$ *vs* $T$ is plotted in Fig. 9. At low temperatures $S$ rises due to $R$ increase and $J$ decrease. When temperature rises $R$ passes though maximum and then decreases. Since $J$ also decreases, the well known $S(T)$ plateau[7] is observed. At elevated temperatures $J$ decreases more rapidly than $R$ so $S$ rises again.

Before the plateau a maximum of $S(T)$ is often observed for $YBa_2Cu_3O_{7-\delta}$ films[11,32] in the temperature range where the $J_1$ component exists. As seen in Figs. 8 and 9, the $S(T)$ peak is pronounced for sample Y4 having large $J_1$ and small $J_2$ but it is absent for sample Y3 having an inverse ratio of the components. Therefore we suppose that the peak is caused by fast relaxation of the $J_1$ component. Because of field suppression of both $R$ and $J_2$ (see Figs. 4 and 7), value of $S \simeq R/J_2$ at the plateau depends on $H$ and proves to be smallest in self-field. At the same time, $H$ slightly affects $J_1$ and amplitude of $R(T)$ maximum therefore field influence on $S(T) = R/(J_1 + J_2)$ is reduced in the temperature range of the peak location. As a result, the peak is more pronounced in self-field as illustrated in bottom panel of Fig. 9.

In Ref. 11 the peak was attributed to a synergetic combination of two types of pinning centers present in the films, namely artificial columnar $BaZrO_3$ inclusions aligned along $c$ axis and the $Y_2O_3$ nanoparticles horizontally aligned in $ab$ plane. There are no artificial inclusions in our films. As discussed below, pinning in our samples is apparently produced by the $Y_2O_3$ participates and oxygen vacancies. Therefore we suppose that the $S(T)$ peak is caused by combination of these pinning centers inherent to $YBa_2Cu_3O_{7-\delta}$ films.

As seen in Figures 4 and 9, the relaxation rates $R$ and $S$ extrapolated to zero temperature don't vanish. The extrapolated $S$ well agrees with the value obtained for $YBa_2Cu_3O_{7-\delta}$ single crystal at $T < 1$ K.[33] The nonzero rate is caused by the quantum tunneling of vortices which occurs in layered superconductors.[3,7] In $YBa_2Cu_3O_{7-\delta}$ films the quantum creep affects vortices dynamics at temperatures up to $5 - 10$ K.[34–36] Precise torque measurements of $YBa_2Cu_3O_{7-\delta}$ single crystal, which revealed a crossover to two-dimensional superconducting behavior at $T < 80$ K,[37] as well as the quantum creep testify importance of layered structure for superconductivity in $YBa_2Cu_3O_{7-\delta}$.

Let's consider now the theoretical basis for two-component current in $YBa_2Cu_3O_{7-\delta}$ films. In Appendix we reduced the general solution of OI theory[39] for the case of magnetic field applied normally to the superconducting planes and calculated the critical current density

$$J_c = J_{c1} + J_{c2},$$

$$J_{c1} = J_p\left[1 - \exp\left\{-a_1\frac{(J_p/J_0)^{5/4}n_p s^{5/4}\xi^{3/4}}{[\varepsilon^2 b\ln(1/b)]^{5/8}}\right\}\right], \quad (5)$$

$$J_{c2} = a_2 J_0\frac{(F_v/\varepsilon_0)^{9/4}n_v\xi^3}{[\varepsilon^2 b\ln(1/b)]^{5/8}}, \quad (6)$$

$$J_0 = J_0(0)\tau_-^{3/2}\tau_+^{1/2}, \qquad b = \xi^2 B/\Phi_0,$$

$$J_0(0) = \frac{c\Phi_0}{12\sqrt{3}\pi^2\xi_0\lambda_0^2} \simeq 300\ \mathrm{MA/cm^2}.$$

The current component $J_{c1}$ is produced by pinning in the superconducting layers. Here $J_p \equiv cF_p/\Phi_0 s$ is the characteristic in-plane current density, $F_p$ and $n_p$ are values of maximal pinning force and concentration of point pinning centers, $s$ is a distance between the planes, $\Phi_0$ is the magnetic flux quantum, and $a_1 = 0.5203$ is the numerical factor. The component $J_{c2}$ is caused by an anisotropic pinning in the superconductor volume. Here

$F_v$ and $n_v$ are values of maximal pinning force and concentration of pinning centers, $\varepsilon_0 = (\Phi_0/4\pi\lambda)^2$ determines the self-energy of the vortex-lines, and $a_2 = 0.9273$ is the numerical factor. Both components depend on the depairing current density $J_0$ (A.5), dimensionless reduced magnetic field $b$ and the anisotropy parameter $\varepsilon$. Using $\lambda_0 = 1400$ Å,[73,74] $\xi_0 = 17.2$ Å[75] we estimated $J_0$ at $T = 0$ for $YBa_2Cu_3O_{7-\delta}$.

As mentioned above, the field dependence of the $J_1$ component of the measured current is weak. For example, at $T = 0$ for sample Y1 we obtained the same value $J_1(0) = 8.0$ MA/cm$^2$ with accuracy of 0.6% for all fields. Let us estimate $J_{c1}$ from its field dependence using the ratio $J_{c1}(B_1)/J_{c1}(B_2) \lesssim 1.01$ of the order of $J_1(0)$ uncertainty for fields $B_1 = 910$ G and $B_2 = 1530$ G. From (5) we obtained $J_{c1}(B_1)/J_{c1}(B_2) = \{1 - \exp[-xf(b_1)]\}/\{1 - \exp[-xf(b_2)]\}$ where $f(b) = [b\ln(1/b)]^{-5/8}$ and $x = a_1 n_p \xi^2 (sJ_p/\varepsilon\xi J_0)^{5/4}$. Taking the above ratio we calculated $x \gtrsim 0.0851$. For oxygen deficiency $\delta \gtrsim 0.03$ in our films the concentration of randomly distributed vacancies in $CuO_2$ planes is estimated as $n_p = (4/7)\delta/ab \simeq 1.15 \cdot 10^{-3}$ Å$^{-2}$ where $a \simeq 3.82$ Å and $b \simeq 3.89$ Å are the orthorhombic lattice cell parameters.[76] Two distances separate pairs of $CuO_2$ planes in $YBa_2Cu_3O_{7-\delta}$: the intra-pair distance $s_p = 3.37$ Å and the inter-pair one of 8.32 Å.[76] Using $s = 8.32$ Å and $\varepsilon = 1/6.5$ (Ref. 77) we estimated lower limits for both the ratio $J_p/J_0 \gtrsim 0.177$ and the current $J_{c1} \gtrsim 53$ MA at $T = 0$.

As follows from the estimation, a weak field dependence of $J_{c1}$ is realized for large currents which are much more than $J_1(0)$. $J_{c1}$ is really more than $J_1$ due to the quantum creep, but at $T \to 0$ the relaxation rate is small (see Fig. 9) and a difference between $J_{c1}(0)$ and $J_1(0)$ must also be small. Thus the field dependence of $J_{c1}$ following from expression (5) contradicts to that of $J_1$. The failure is caused by high concentration of defects in the $CuO_2$ planes. Since a number of defects per square of vortex core exceeds unity, $N_p \simeq \pi\xi^2 n_p \simeq 1.07$, the core contains a defect at any site. In such conditions only fluctuations of defect density pin vortices and the pinning becomes *collective*[3,38] while expression (5) is obtained for *strong* pinning.

In the case of the collective pinning the current is independent of field in the single-vortex pinning regime which is realized if $s < L_c^c < \varepsilon a_0$. In magnetic field directed along the $c$ axis a length of the collective pinning segment for $YBa_2Cu_3O_{7-\delta}$ is estimated as $L_c^c \simeq 10\varepsilon\xi_0 \simeq 26.5$ Å.[3] Both an inter-vortex distance $a_0 \simeq (2\Phi_0/\sqrt{3}B)^{1/2} \gtrsim 1100$ Å and its product $\varepsilon a \gtrsim 170$ Å exceeded $L_c^c$ in our experiments so conditions for field independence of the current were fulfilled. Therefore we suppose that in-plane pinning is produced by the collective action of oxygen vacancies. Let us compare $J_1$ with $J_c$ obtained in CP theory for a layered superconductor.

In field applied along normal to superconducting planes the critical current coincides for layered and anisotropic superconductors. For single vortex collective

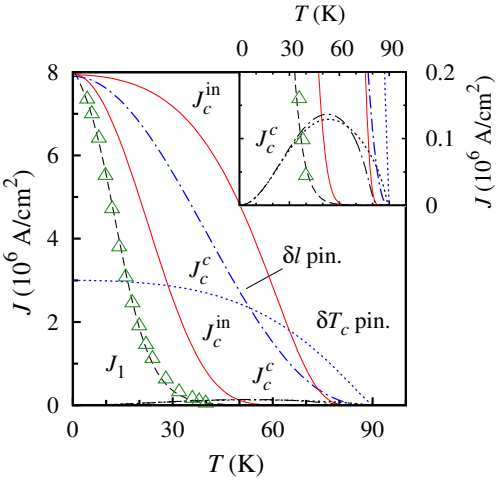


FIG. 10. (Color online) $J_1(T)$ obtained in self-field for sample Y1 (triangles) and its approximations by Eq. (4) — dashed line, $J_c^{\rm in}$ Eq. (11) — continuous lines (left for $\beta = 0.62$ and right for $\beta = 0.1$), $J_c^c$ Eqs. (7) and (9) — dotted lines for $\delta T_c$ pinning and dash-dotted lines for $\delta\ell$ pinning. The currents are magnified in inset to illustrate $J_c^c(T)$ following from Eqs. (9).

pinning it is expressed as[3]

$$J_c^c = J_0\left[\frac{\delta_m}{\varepsilon}\right]^{2/3} = J_0(0)\left[\frac{\delta_m(0)}{\varepsilon}\right]^{2/3}\tau_+^{-1/2}\tau_-^{5/2} \quad \delta\ell \text{ pin.} \quad (7a)$$

$$J_c^c = J_0\left[\frac{\delta_\alpha}{\varepsilon}\right]^{2/3} = J_0(0)\left[\frac{\delta_\alpha(0)}{\varepsilon}\right]^{2/3}\tau_+^{5/6}\tau_-^{7/6} \quad \delta T_c \text{ pin.} \quad (7b)$$

The dimensionless pinning parameters for oxygen vacancies in $YBa_2Cu_3O_{7-\delta}$ are estimated as $\delta_m(0)/\varepsilon \simeq (0.2-1)10^{-2}$ for $\delta\ell$ pinning and $\delta_\alpha(0)/\varepsilon \simeq 10^{-3}$ for $\delta T_c$ pinning,[3] and the corresponding currents are $J_c^c(0) \simeq (5-14)$ MA/cm$^2$ and $J_c^c(0) \simeq 3$ MA/cm$^2$. The dependence $J_1(T)$ obtained in self-field for sample Y1 as well as fitting curves for Eqs. (7) are presented in Fig. 10. As seen $J_1(T)$ disagree with $J_c^c(T)$ curves, moreover for $\delta T_c$ pinning the current $J_c^c(0)$ is about two times lower than $J_1(0)$.

Eqs. (7) does not take into account thermal fluctuations suppressing the critical current at high temperatures[3]

$$J_c^c = \frac{c(k_{\rm B}T)^2}{\Phi_0\varepsilon_0\xi^3}\exp\left[-\frac{3w}{2\delta_{\alpha,m}}\left(\frac{k_{\rm B}T}{\varepsilon_0\xi}\right)^3\right]. \quad (8)$$

Here $w$ is a factor of the order of unity. Selecting tem-

perature dependences of quantities[65] we write

$$J_c^c = J_c^c(0)\frac{\tau^2\tau_-^{1/2}}{\tau_+^{5/2}}\exp\left[-\frac{3w}{2}\left(\frac{T}{T^*}\right)^3\frac{1}{f_c^c(T)}\right], \quad (9)$$

$$f_c^c(T) = \begin{cases}\tau_+^3\tau_-^3 & \text{for } \delta\ell \text{ pinning},\\ \tau_+^5\tau_- & \text{for } \delta T_c \text{ pinning},\end{cases}$$

$$J_c^c(0) = \frac{3\sqrt{3}}{4}J_0(0)\left[\frac{k_\mathrm{B}T_c}{\varepsilon_0(0)\xi_0}\right]^2 \simeq 1.07 \text{ MA/cm}^2,$$

$$T^* = \frac{\varepsilon_0(0)\xi_0\delta_{\alpha,m}^{1/3}(0)}{k_\mathrm{B}} \simeq \begin{cases}(198-116) \text{ K} & \delta\ell \text{ pin.},\\ 92 \text{ K} & \delta T_c \text{ pin.}\end{cases}$$

Due to fluctuations the current is strongly suppressed at temperatures above the depinning temperature which is calculated from the equation $T_\mathrm{dp}^3 = T^{*3}f_c^c(T_\mathrm{dp})$.[3] The temperatures $T_\mathrm{dp} \simeq 89$ K and 71–79 K calculated for $\delta T_c$ and $\delta\ell$ pinning are considerably higher than temperatures at which $J_1$ disappears. In Fig. 10 dependences (9) are shown. As seen, a magnitude of $J_1(T)$ a lot more than maximal values of $J_c^c(T)$ and the curves lie in different temperature ranges. Thus we conclude that neither Eqs. (7) nor (9) describe $J_1$ component of the measured current.

In magnetic field parallel to a superconducting layers the intrinsic pinning takes place in a layered superconductor.[3,78,79] Kinks of vortices[80,81] also lead to the intrinsic pinning. Though our experiments were performed in a transverse field, a demagnetizing effect, which was strong because of low fields and large demagnetizing factor of films, produced a tangential component of field[82] directed along superconducting layers in the films. Therefore the critical current produced by the intrinsic pinning should be also considered. Its temperature dependence has the form[3,79]

$$J_c^\mathrm{in} = J_0\left(\frac{8\varepsilon\xi}{s}\right)^2\left(1-\frac{B}{B_{c2}}\right)\exp\left[-8\left(\frac{\varepsilon\xi}{s}\right)^2\right]. \quad (10)$$

Neglecting the field dependence, since $B \ll B_{c2}$ in our experiments, we write it as

$$J_c^\mathrm{in} = 64\beta J_0(0)\tau_+^{3/2}\tau_-^{1/2}\exp[-8\beta\tau_+/\tau_-], \quad (11)$$
$$\beta = (\varepsilon\xi_0/s)^2 = 0.62-0.1.$$

Here we estimated $\beta$ for the above mentioned distances between $CuO_2$ planes. $J_c^\mathrm{in}(T)$ curves calculated for $\beta = 0.62$ and 0.1 and normalized by factors 0.094 and 0.0092 respectively are presented in Fig. 10. While quasi-exponential shape of $J_c^\mathrm{in}(T)$ is more appropriate to $J_1(T)$, the intrinsic current decreases more slowly and disappears at higher temperatures. In addition at low temperatures $J_c^\mathrm{in}$ is one or two orders more than $J_1$.

Summing up we conclude that $J_1$ component of the current is caused by the collective pinning of vortices on oxygen vacancies in the single vortex pinning regime. However we failed to find an appropriate approximation for $J_1(T)$ in the frame of CP theory. Apparently, because of smallness of pinning energy, $J_1$ rapidly relaxes and its temperature dependence is strongly affected by creep.

Turning to volume pinning we begin with a remark about pinning on the dislocations. In EDP model[14] the critical current depends on an average size of the crystallites, i. e. CDB size in the diffraction experiments, as well as on a misorientation angle $\omega$ between them.[42] As seen in Table I, in our samples the CDB size changes by one order and the angle $\omega$ varies almost seven times, but these parameters do not correlate with $J_2$. Despite absence of the correlation, we compare below $J_2(T)$ with $J_c(T)$ calculated for pinning on both non-superconducting inclusions and the edge dislocations for analysis to be comprehensive.

In low fields the critical current of $YBa_2Cu_3O_{7-\delta}$ films is independent of field.[10,12,19,21,23,64]

The field-independent current produced by pinning on the edge dislocations is calculated as[14]

$$J_{cd}(T,0) \simeq \frac{3\sqrt{3}}{16\sqrt{2}}\frac{c\varepsilon_0}{\Phi_0}\frac{r_d^2}{\xi^3} = J_{cd}^0\left(\frac{r_d}{\xi_0}\right)^2\frac{\tau_-^{5/2}}{\tau_+^{1/2}}, \quad (12)$$
$$J_{cd}^0 = \frac{27}{64\sqrt{2}}J_0(0) = 89.5 \text{ MA/cm}^2,$$

where $r_d$ is the radius of dislocation normal core. Dependences $J_2(T)$ obtained in self-field and their fits by Eqs. (12) are presented in Fig. 11. From the fits we obtained $r_d \simeq 4.6$, 5.0, 5.3 and 4.6 Å respectively for samples Y1–Y4. Eq. (12) provides the same temperature dependence for all samples scaled by $r_d$ values while $J_2(T)$ curves differ for different samples. The dependence $J_{cd}(T,0)$ satisfactory approximates $J_2(T)$ only for sample Y1 while for other ones a discrepancy of the fitting curves and the experimental data is clearly seen at $T/T_c \gtrsim 0.5$.

The field-independent current caused by pinning on inclusions[19]

$$J_{ci}(T,0) \simeq \frac{3J_0}{4}\sqrt{\frac{3n_i}{\pi\varepsilon^2}}\left(\frac{F_i\xi}{\varepsilon_0}\right)^{3/2}$$

depends on inclusion density $n_i$ and the pinning force $F_i$ approximated as[3,19]

$$\frac{F_i\xi}{\varepsilon_0} \simeq \frac{D_{iz}}{4}\mathcal{F}(T,d_i),$$
$$\mathcal{F}(T,d_i) = \ln\left(1+\frac{D_i^2}{2\xi^2}\right) = \ln\left(1+\frac{d_i^2\tau_-}{2\tau_+}\right). \quad (13)$$

Here $D_i$ is an average extent of an inclusion, $D_{iz}$ is its extent along the field direction and $d_i = D_i/\xi_0$. Selecting temperature dependences of quantities we write the current in the form

$$J_{ci}(T,0) \simeq J_{ci}^0[\mathcal{F}(T,d_i)\tau_-]^{3/2}\tau_+^{1/2}, \quad (14)$$
$$J_{ci}^0 \simeq \frac{3\sqrt{3}}{32\sqrt{\pi}}\frac{J_0(0)}{\varepsilon}\sqrt{n_iD_{iz}^3} \simeq \sqrt{n_iD_{iz}^3}\cdot 179 \text{ MA/cm}^2.$$

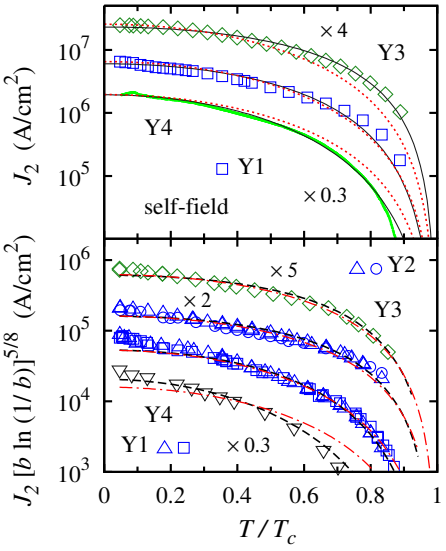


FIG. 11. (Color online) *Top:* $J_2(T)$ for $YBa_2Cu_3O_{7-\delta}$ films obtained in self-field. Experimental curve for sample Y4 was recorded under warming of film right after magnetic field removing. Dotted and continuous lines are fits by dependences (12) and (14). *Bottom:* Scaled $J_2(T)$ dependences obtained in fields 1530 Oe (triangles) and 910 Oe (other symbols). Dashed and dash-dotted lines are fits by dependences (17) and (15). The curves are shifted (multiplied by shown factors) to avoid a crossing. See text for details.

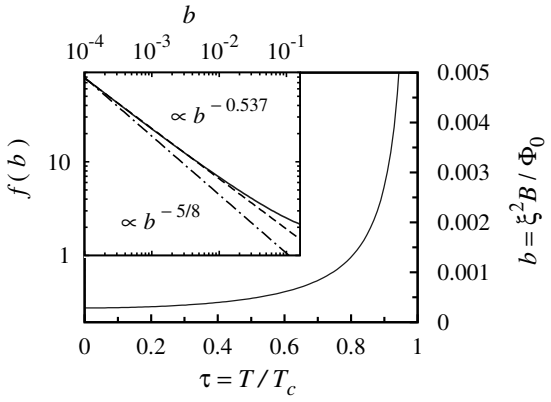


FIG. 12. Temperature dependence of the parameter $b = B\xi^2/\Phi_0 = B\xi_0^2\tau_+/\Phi_0\tau_-$ calculated for $B = 2$ kG and $\xi_0 = 17.2$ Å. *Inset:* function $f = [b\ln(1/b)]^{-5/8}$ (continuous line) and its approximations $f = 0.5552\cdot b^{-0.537}$ (dashed), $f = 0.25\cdot b^{-5/8}$ (dash-dot).

$J_2(T)$ curves were fitted by the dependence (14) via parameters $J_{ci}^0$ and $D_i$. The currents $J_{ci}^0 = 2.7$, 1.1 0.88 and 25 MA/cm$^2$ were respectively obtained for samples Y1–Y4. $D_i$ values are presented in Table I. The fitting curves shown in Fig. 11 well agree with $J_2(T)$ for samples Y1 and Y3 though for Y1 the measured current decays more slowly at $T/T_c \gtrsim 0.75$. For sample Y4 the measured and fitting curves coincide up to $T \sim T_{\rm dp}$.

Thus pinning on inclusions well describes $J_2(T)$ of $YBa_2Cu_3O_{7-\delta}$ films in self-field. Interaction of vortices suppresses the critical current when a vortex density $\tilde{n} \simeq B/\Phi_0$ increases. Let us proceed with analysis of field dependence of $J_{c2}$ which is determined by the function $f = [b\ln(1/b)]^{-5/8}$, see Eq. (6). Because of large $B_{c2}$ in $YBa_2Cu_3O_{7-\delta}$ the parameter $b = B/2\pi B_{c2}$ is small. In Figure 12 we plotted $b(T)$ for $B = 2$ kG exceeding maximum field in our experiments. As seen, $b$ is less than 0.005 for $T/T_c \lesssim 0.95$. In the inset of Fig. 12 the function $f$ is plotted in the range up to $b = 1/2\pi$ corresponding to $B = B_{c2}$. For small $b$ it follows a power law and in the range $10^{-4} \le b \le 0.005$ is approximated as $f = 0.5552\cdot b^{-0.537}$ with the accuracy of $\pm 1.2\%$. The dependence $J \propto B^{-\alpha}$ with $\alpha \simeq 0.4$–$0.8$ was often observed for $YBa_2Cu_3O_{7-\delta}$ films[10,12,19,21,23,52,64] and 2G-tapes.[9]

As seen in Fig. 12, at $b \gtrsim 0.01$ the function $f(b)$ moderates and should be approximated by $f \propto b^{-\alpha}$ with a lower $\alpha$. However strengthening $J(B)$ dependence in high fields was reliably established for $YBa_2Cu_3O_{7-\delta}$ films in numerous experiments.[11,12,19–21,23,28,64] Expression (6) is valid only if the lateral displacement of the vortex lines $u_0$ is small in comparison with the inter-vortex distance $a_0$. In high fields when $a_0 \propto B^{-1/2}$ becomes larger than $u_0$ a more strong suppression of the current $J_{c2} \propto B^{-1}$ is expected.[19]

According to Eq. (6) the curves $J_{c2}[b\ln(1/b)]^{5/8}$ should be independent of field. Indeed, as seen in bottom Fig. 11, the data obtained for samples Y1 and Y2 in different fields are joined into common curves under such scaling. Therefore we compare $J_c(T,B)[b\ln(1/b)]^{5/8}$ dependences with the scaled data collected for different fields.

In the EDP model the field-dependent critical current[14]

$$J_{cd}(T,B) = J_{cd}(T,0)\frac{\tilde{n}_p}{\tilde{n}}, \qquad (15)$$

$$\frac{\tilde{n}_p(T,B)}{\tilde{n}(B)} = 1 - \frac{[\Gamma(\nu,\eta) - \eta\Gamma(\nu-1,\eta)]^2}{\Gamma^2(\nu)},$$

$$\nu = \left[\frac{\langle L\rangle}{\sigma}\right]^2, \quad \eta(T,B) = \frac{r_d}{\langle L\rangle}\frac{2\nu}{\xi_0}\sqrt{\frac{\Phi_0}{B}\frac{\tau_-}{\tau_+}}, \qquad (16)$$

is determined by a relative number of pinned vortices $\tilde{n}_p/\tilde{n}$ expressed via complete and incomplete Euler's gamma functions $\Gamma(x)$ and $\Gamma(x,y)$.[83] Here $\sigma$ is the dispersion of the crystallite size distribution function around the mean value $\langle L\rangle$.

The scaled currents were fitted by $J_{cd}(T,B)[b\ln(1/b)]^{5/8}$ via $J_{cd}(0,0)$, $\nu$ and $\eta$ using $B = 910$ G as parameter. The fitting curves, shown in bottom Fig. 11, agree with experimental data for samples Y1–Y3 though a systematic deviation to a lower current is observed at low temperatures. At the same time the fit badly approximates data for sample Y4. From the fit we obtained $\eta \simeq 2$ for all samples, $\nu \simeq 7$ for Y2, Y3 and $\nu \simeq 1$ for Y1, Y4. Then from (16) for $B = 910$ G the ratio $r_d/\langle L\rangle$ was estimated as $1.1\cdot 10^{-2}$ for samples Y2, Y3 and $1.6\cdot 10^{-3}$ for Y1,Y4. From

$J_{cd}(0,0)$ values we calculated $r_d$ and then obtained $\langle L\rangle$ presented in Table I. As seen, the fit gives a correct order for $r_d$ and $\langle L\rangle$ values, however lengths $\langle L\rangle$ does not correlate with average sizes of crystallites CDB obtained in the diffraction experiments. Neither $r_d$ nor $\langle L\rangle$ correlate with the measured current $J$ or its components.

For pinning on inclusions the field-dependent current calculated from Eqs. (6) and (13) takes the form[84]

$$J_{ci}(T,B) \simeq \frac{J_{ci}^B}{[b\ln(1/b)]^{5/8}}\mathrm{F}(T,d_i), \tag{17a}$$

$$\mathrm{F}(T,d_i) = \ln^{9/4}\left(1+\frac{d_i^2\tau_-}{2\tau_+}\right)\tau_-^{9/8}\tau_+^{7/8}, \tag{17b}$$

$$J_{ci}^B = \frac{3^{3/4}J_0(0)n_iD_{iz}^{9/4}\xi_0^{3/4}}{16\cdot 2^{3/4}\pi^{5/8}\varepsilon^{5/4}} \simeq n_iD_{iz}^{9/4}\xi_0^{3/4}\cdot 129\ \mathrm{MA/cm^2},$$

The scaled currents were fitted by the dependence $J_{ci}^B\mathrm{F}(T,d_i)$ via $J_{ci}^B$ and $D_i$. Since size of inclusions is independent of field, we used the same $D_i$ to fit $J_2$ by both (14) and (17). An effective density of inclusions $n_id_{iz}^{9/4} = n_i(D_{iz}/\xi_0)^{9/4}$ was calculated from $J_{ci}^B$ values. The fitting curves $J_{ci}^B\mathrm{F}(T,d_i)$, presented in bottom Fig. 11, agree with experimental data for all samples.

Obtained $D_i$ and $n_id_{iz}^{9/4}$ values are presented in Table I. The average extent of inclusions $D_i$ varying in the range $2-14$ nm well agrees with size of $Y_2O_3$ precipitates in $YBa_2Cu_3O_{7-\delta}$ films.[15–18] $D_i$ and $n_id_{iz}^{9/4}$ values correlate with $J_2$ component of the current. The larger inclusion extent the more $J_2$. For inclusions with the same $D_i$ the current rises with increase of the effective inclusion density $n_id_{iz}^{9/4}$.

As follows form Eqs. (14) and (17), the extent of inclusion along the field direction can be obtained from the ratio $(J_{ci}^0)^2/J_{ci}^B = (D_{iz}/\xi_0)^{3/4}\cdot 248$ A/cm$^2$. Then $n_i$ is simply calculated from $J_{ci}^B$ or $J_{ci}^0$. Values of $D_{iz}$ and $n_i$ found in such a procedure are presented in Table I.

Parameters of pinning centers obtained for our films well agree with $D_i = 15$ nm and $n_i = (1-3)\cdot 10^{15}$ cm$^{-3}$ found in magnetic experiments in Ref. 19. At the same time a lower density of inclusions was found in direct measurements by means of the electron microscopy.[15–18]

Among microstructure defects in $YBa_2Cu_3O_{7-\delta}$ films[10,17,18] the precipitates[15–18] [001]-$Y_20_3$ and [110]-$Y_20_3$ have dimensions close to our estimations of $D_i$. The [110]-$Y_20_3$ precipitates are small cubes or rectangles with sides ranging from 3 to 5 nm.[18] The [001]-$Y_20_3$ precipitates have extension of 10 to 20 nm in the $ab$-plane and about 6 to 8 nm along the $c$ axis.[15–18] There are no data on density and shape of inclusions with size smaller than 2 nm since such small inclusions are hard to recognize even in high-resolution electron microscopy (HREM) micrographs.[17,18] Our results for sample Y4 demonstrate presence of such inclusions which we classified as the [110]-$Y_20_3$ precipitates. Taking $D_{iz} = D_i$ for samples Y1, Y4 and $D_{iz} = 6$ nm for Y2, Y4, from the effective density of inclusions obtained above we estimated densities $n_i^*$ presented in Table I. For samples Y1–Y3 estimated $n_i^*$ values are only twice less than that observed by direct HREM method in laser-deposited $YBa_2Cu_3O_{7-\delta}$ films.[18] Since a density of $Y_20_3$ precipitates depends on both method and conditions of the deposition process[10,11,17,18] such agreement seems quite satisfactory. Note also that the measured relaxed persistent current is less than $J_c$ so a lower limit for the inclusion densities was estimated in our experiment.

Summing up we conclude that the $J_2$ component of the measured current is well described by pinning on the $Y_20_3$ inclusions. The pinning is strong and its efficiency rises with increase of inclusions size.

## V. SUMMARY

In this paper we confirmed experimentally that the critical current of laser-deposited $YBa_2Cu_3O_{7-\delta}$ films consists of two components caused by in-plane pinning of vortices by oxygen vacancies in superconducting $CuO_2$ planes and by anisotropic pinning on the $Y_20_3$ precipitates in the superconductor volume.[39] We proposed a simple method to separate the current components and found their temperature dependences (3) and (4). Analysis of the current components led us to the following conclusions.

The component produced by the in-plane pinning is described as single-vortex collective pinning however we failed to find an appropriate theoretical dependence to approximate its temperature behavior. This component slightly depends on field and rapidly relaxes. The in-plane pinning is substantial only at low temperatures $T \lesssim 30$ K but in this temperature range its contribution into the critical current and vortices dynamics should not be neglected.

The component produced by the volume pinning is well described in the frame of OI theory[39] further developed by van der Beek *et al.*[19] We confirmed that in laser-deposited $YBa_2Cu_3O_{7-\delta}$ films the strong anisotropic volume pinning is produced by the nano-size $Y_2O_3$ precipitates. Varying inclusion sizes in different films causes difference in the depinning temperatures and parameters of $J(T)$ dependence. Rather low magnetic field of about 1 kOe applied normally to the film plane affects this current component.

Different ratio of the current components and variation of size of the $Y_2O_3$ inclusions lead to a wide variety of $J(T)$ dependences in standard $YBa_2Cu_3O_{7-\delta}$ films. Addition of artificial defects further complicates $J(T,\mathbf{B})$ behavior. Nevertheless films produced by different techniques demonstrate some common features discussed in beginning Sec. III.

While in-plane and volume defects act simultaneously and provide additive components of the current, combining several types of volume defects is not simply additive. Therefore engineering the pinning landscape in 2G/3G-tapes is a very complex problem.[10,11] We hope that sep-

aration and correct analysis of the additive components demonstrating strongly different temperature, field and angle behavior help in solving this actual problem.

## Appendix

An inhomogeneous layered superconductor with an axial anisotropy and the mass anisotropy ratio $\varepsilon^2 = m/M = \lambda/\lambda_c$ was considered by Ovchinnikov and Ivlev.[39] Here $m$ and $\lambda$ are the effective mass of carriers and the penetration depth in isotropic superconducting planes and $M$, $\lambda_c$ are the corresponding parameters along normal to the planes. General case of magnetic field $B$ applied along the direction forming an angle $\theta$ with the planes was analyzed and the critical current density was calculated. We simplify the results obtained by Ovchinnikov and Ivlev for the case $\theta = \pi/2$, when the field is directed normally to the planes, and rewrite the values in the notations of Ref. 3 commonly used at present.

As shown by Ovchinnikov and Ivlev, the critical current consists of two parts

$$J_c = J_{c1} + J_{c2} \tag{A.1}$$

caused by in-plane pinning on point defects in the superconducting planes and by anisotropic pinning of vortices by "macro-defects" in the superconductor volume.

The anisotropic component of the current is written as follows[39]

$$J_{c2} = \frac{cn_v F_v^2}{\Phi_0 \alpha^2 \sqrt{\epsilon_{xx} C_{xx}}} \left[ \frac{128 F_v \xi^3}{27\sqrt{\epsilon_{yy} C_{yy}}} \right]^{1/4}, \tag{A.2}$$

where $F_v$ and $n_v$ are maximum values of pinning force and concentration of pinning centers in volume of the superconductor, $\xi$ is the in-plane coherent length, $\Phi_0$ is the magnetic flux quantum. Taking into account the units $\hbar = c = 1$ used by Ovchinnikov and Ivlev[39] we multiplied the right hand side by the light velocity $c$. The function $\alpha^2 = \sin^2\theta + \varepsilon^2 \cos^2\theta$ is equal to unity in our case. The quantities

$$C_{yy} = \alpha^2 C_{xx} = C_{xx} = \frac{\Phi_0 B}{8\pi\lambda^2} = \frac{2\pi b \varepsilon_0}{\xi^2} \tag{A.3}$$

we express via the energy $\varepsilon_0 = (\Phi_0/4\pi\lambda)^2$ which determines the self-energy of the vortex-lines[3] and the parameter $b = \xi^2 B/\Phi_0$. The quantities $\epsilon_{xx}$ and $\epsilon_{yy}$ are written as

$$\epsilon = \frac{\Phi_0^2}{8\pi^2\lambda^2} \ln\left[ \frac{\sqrt{\alpha\Phi_0/B}}{d\cos\theta + \alpha\xi} \right] \tilde{\epsilon} = \varepsilon_0 \ln(1/b)\tilde{\epsilon}. \tag{A.4}$$

From bulky but simple expressions for $\tilde{\epsilon}_{xx}(\theta, \varepsilon)$ and $\tilde{\epsilon}_{yy}(\theta, \varepsilon)$ in Ref. 39 we calculated that in our case $\tilde{\epsilon}_{xx} = \tilde{\epsilon}_{yy} = \tilde{\epsilon} = \varepsilon^2/2$.

Substituting all obtained values in (A.2), and using expression for the depairing current density[3]

$$J_0 = \frac{4}{3\sqrt{3}} \frac{c\varepsilon_0}{\Phi_0 \xi}, \tag{A.5}$$

after simple algebraic transformations we get the anisotropic component of the critical current density in the form

$$J_{c2} = a_2 J_0 \left( \frac{F_v}{\varepsilon_0} \right)^{9/4} \frac{n_v \xi^3}{[\varepsilon^2 b \ln(1/b)]^{5/8}}, \qquad a_2 = \frac{3^{3/4}}{2^{1/4}\pi^{5/8}} = 0.9373. \tag{A.6}$$

The current component caused by the layered structure of superconductor is written as[39]

$$J_{c1} = \frac{cF_p}{\Phi_0 s} \left[ 1 - \exp\left\{ -\frac{n_p F_p}{\sin\theta\sqrt{\epsilon_{xx} C_{xx}}} \left( \frac{128 F_p \xi^3}{27\sqrt{\epsilon_{yy} C_{yy}}} \right)^{1/4} \right\} \right], \tag{A.7}$$

where $F_p$ and $n_p$ are maximum values of pinning force and concentration of pinning centers in the superconducting planes, $s$ is a distance between the planes. Substituting all values obtained above, taking into account that $\sin\theta = 1$ in our case and denoting $J_p = cF_p/(\Phi_0 s)$, after simple algebraic transformations we rewrite (A.7) as

$$J_{c1} = J_p \left[ 1 - \exp\left\{ -a_1 \left( \frac{J_p}{J_0} \right)^{5/4} \frac{n_p s^{5/4} \xi^{3/4}}{[\varepsilon^2 b \ln(1/b)]^{5/8}} \right\} \right], \qquad a_1 = \frac{16 \cdot 2^{1/4}}{9 \cdot (3\pi)^{5/8}} = 0.5203. \tag{A.8}$$


## ACKNOWLEDGMENTS

The authors would like to thank O. A. Krymskaya for the structure measurements, O. A Churkin for technical assistance and A. P. Menushenkov for fruitful discussions. The work was supported by Russian Science Foundation

grant 14-22-00098.


[1] A. M. Campbell and J. E. Evetts, Adv. Phys. **21**, 199 (1972).
[2] A. I. Larkin and Y. N. Ovchinnikov, J. Low Temp. Phys. **34**, 409 (1979).
[3] G. Blatter, M. V. Feigel'man, V. B. Geshkenbein, A. I. Larkin, and V. M. Vinokur, Rev. Mod. Phys. **66**, 1125 (1994).
[4] E. H. Brandt, Rep. Prog. Phys. **58**, 1465 (1995).
[5] M. V. Feigel'man and V. M. Vinokur, Phys. Rev. B **41**, 8986 (1990).
[6] D. R. Nelson and V. M. Vinokur, Phys. Rev. B **48**, 13060 (1993).
[7] Y. Yeshurun, A. P. Malozemoff, and A. Shaulov, Rev. Mod. Phys. **68**, 911 (1996).
[8] A. P. Malozemoff, S. Fleshler, M. Rupich, C. Thieme, X. Li, W. Zhang1, A. Otto, J. Maguire, D. Folts, J. Yuan, H.-P. Kraemer, W. Schmidt, M. Wohlfart, and H.-W. Neumueller, Supercond. Sci. Technol. **21**, 034005 (2008).
[9] C. Senatore, C. Barth, M. Bonura, M. Kulich, and G. Mondonico, Supercond. Sci. Technol. **29**, 014002 (2016).
[10] S. R. Foltyn, L. Civale, J. L. MacManus-Driscoll, Q. X. Jia, B. Maiorov, H. Wang, and M. Maley, Nat. Mater. **6**, 631 (2007).
[11] B. Maiorov, S. A. Baily, H. Zhou, O. Ugurlu, J. A. Kennison, P. C. Dowden, T. G. Holesinger, S. R. Foltyn, and L. Civale, Nat. Mater. **8**, 398 (2009).
[12] B. Dam, J. M. Huijbregtse, F. C. Klaassen, R. C. F. van der Geest, G. Doornbos, J. H. Rector, A. M. Testa, S. Freisem, J. C. Martinez, B. Stäuble-Pümpin, and R. Griessen, Nature **399**, 439 (1999).
[13] J. M. Huijbregtse, B. Dam, R. C. F. van der Geest, F. C. Klaassen, R. Elberse, J. H. Rector, and R. Griessen, Phys. Rev. B **62**, 1338 (2000).
[14] V. Pan, Y. Cherpak, V. Komashko, S. Pozigun, C. Tretiatchenko, A. Semenov, E. Pashitskii, and A. V. Pan, Phys. Rev. B **73**, 054508 (2006).
[15] A. Catana, R. F. Broom, J. G. Bednorz, J. Mannhart, and D. G. Schlom, Appl. Phys. Lett. **60**, 1016 (1992).
[16] T. I. Selinder, U. Helmersson, J.-E. S. Z. Hart, H. Sjöström, and L. R. Wallenberg, Physica C **202**, 69 (1992).
[17] G. Kästner, D. Hesse, R. Scholz, H. Koch, F. Ludwig, M. Lorenz, and H. Kittel, Physica C **243**, 281 (1995).
[18] K. Verbist, A. Kühle, and A. L. Vasiliev, Physica C **269**, 131 (1996).
[19] C. J. van der Beek, M. Konczykowski, A. Abal'oshev, I. Abal'osheva, P. Gierlowski, S. J. Lewandowski, M. V. Indenbom, and S. Barbanera, Phys. Rev. B **66**, 024523 (2002).
[20] A. O. Ijaduola, J. R. Thompson, R. Feenstra, D. K. Christen, A. A. Gapud, and X. Song, Phys. Rev. B **73**, 134502 (2006).
[21] M. Miura, B. Maiorov, S. A. Baily, N. Haberkorn, J. O. Willis, K. Marken, T. Izumi, Y. Shiohara, and L. Civale, Phys. Rev. B **83**, 184519 (2011).
[22] E. Moraitakis, M. Pissas, G. Kallias, and D. Niarchos, Supercond. Sci. Technol. **12**, 682 (1999).
[23] M. Peurla, H. Huhtinen, and P. Paturi, Supercond. Sci. Technol. **18**, 628 (2005).
[24] J. Gutiérrez, T. Puig, and X. Obradors, Appl. Phys. Lett. **90**, 162514 (2007).
[25] T. Puig, J. Gutiérrez, A. Pomar, A. Llordés, J. Gázquez, S. Ricart, F. Sandiumenge, and X. Obradors, Supercond. Sci. Technol. **21**, 034008 (2008).
[26] O. Polat, J. W. Sinclair, Y. L. Zuev, J. R. Thompson, D. K. Christen, S. W. Cook, D. Kumar, Y. Chen, and V. Selvamanickam, Phys. Rev. B **84**, 024519 (2011).
[27] E. A. Pashitskiĭ, V. I. Vakaryuk, S. M. Ryabchenko, and Y. V. Fedotov, Low Temp. Phys. **27**, 96 (2001).
[28] Y. V. Fedotov, S. M. Ryabchenko, E. A. Pashitskiĭ, A. V. Semenov, V. I. Vakaryuk, V. M. Pan, and V. S. Flis, Low Temp. Phys. **28**, 172 (2002).
[29] M. Djupmyr, G. Cristiani, H.-U. Habermeier, and J. Albrecht, Phys. Rev. B **72**, 220507(R) (2005).
[30] J. Albrecht, M. Djupmyr, and S. Brück, J. Phys.: Condens. Matter **19**, 216211(7) (2007).
[31] J. Jung, H. Yan, H. Darhmaoui, M. Abdelhadi, B. Boyce, and T. Lemberger, Supercond. Sci. Technol. **12**, 1086 (1999).
[32] H. Yan, , J. Jung, H. Darhmaoui, Z. F. Ren, J. H. Wang, and W.-K. Kwok, Phys. Rev. B **61**, 11 711 (2000).
[33] L. Fruchter, A. P. Malozemoff, I. A. Campbell, J. Sanchez, M. Konczykowski, R. Griessen, and F. Holtzberg, Phys. Rev. B **43**, 8709 (1991).
[34] A. J. J. van Dalen, R. Griessen, S. Libbrecht, Y. Bruynseraede, and E. Osquiguil, Phys. Rev. B **54**, 1366 (1996).
[35] A. F. T. Hoekstra, A. M. Testa, G. Doornbos, J. C. Martinez, B. Dam, R. Griessen, B. I. Ivlev, M. Brinkmann, K. Westerholt, W. K. Kwok, and G. W. Crabtree, Phys. Rev. B **59**, 7222 (1999).
[36] I. Landau and H. Ott, Physica C **340**, 251 (2000).
[37] D. E. Farrell, J. P. Rice, D. M. Ginsberg, and J. Z. Liu, Phys. Rev. Lett. **64**, 1573 (1990).
[38] G. Blatter, V. B. Geshkenbein, and J. A. G. Koopmann, Phys. Rev. Lett. **62**, 067009 (2004).
[39] Y. N. Ovchinnikov and B. I. Ivlev, Phys. Rev. B **43**, 8024 (1991).
[40] A. Gurevich and E. A. Pashitskii, Phys. Rev. B **57**, 13 878 (1998).
[41] V. M. Pan, E. A. Pashitskii, S. M. Ryabchenko, V. A. Komashko, A. V. Pan, S. X. Dou, A. V. Semenov, C. G. Tretiatchenko, and Y. V. Fedotov, IEEE Trans. Appl. Supercond. **13**, 054508 (2003).
[42] A. I. Kosse, A. Y. Prokhorov, V. A. Khokhlov, G. G. Levchenko, A. V. Semenov, D. G. Kovalchuk, M. P. Chernomorets, and P. N. Mikheenko, Supercond. Sci. Technol. **21**, 075015 (2008).
[43] A. A. Ivanov, S. G. Galkin, A. V. Kuznetsov, and A. P. Menushenkov, Physica C **180**, 69 (1991).
[44] E. V. Pechen, A. V. Varlashkin, S. I. Krasnosvobodtsev, B. Brunner, and K. F. Renk, Appl. Phys. Lett. **66**, 2292 (1995).
[45] V. N. Trofimov, Cyogenics **32**, 513 (1992).
[46] A. V. Kuznetsov, A. A. Ivanov, D. V. Eremenko, and V. N. Trofimov, Phys. Rev. B **52**, 9637 (1995).
[47] I. L. Landau and H. R. Ott, Phys. Rev. B **63**, 184516 (2001).

[48] P. N. Mikheenko and Y. E. Kuzovlev, Physica C **204**, 229 (1993).
[49] J. R. Clem and A. Sanchez, Phys. Rev. B **50**, 9355 (1994).
[50] A. A. Babaei Brojeny and J. R. Clem, Supercond. Sci. Technol. **18**, 888 (2005).
[51] P. Bernstein, J. Appl. Phys. **111**, 103913 (2012).
[52] A. V. Kuznetsov, I. I. Sannikov, A. A. Ivanov, A. P. Menushenkov, and O. A. Churkin, IEEE Trans. Appl. Sup. **26**, 8000505 (2016).
[53] M. R. Beasley, R. Labusch, and W. W. Webb, Phys. Rev. **181**, 682 (1969).
[54] M. Nideröst, A. Suter, P. Visani, A. C. Mota, and G. Blatter, Phys. Rev. B **53**, 9286 (1996).
[55] I. P. Krylov, E. J. Maritz, and E. B. Nyeanchi, Phys. Rev. B **58**, 14609 (1998).
[56] J. R. Thompson, K. D. Sorge, C. Cantoni, H. R. Kerchner, D. K. Christen, and M. Paranthaman, Supercond. Sci. Technol. **18**, 970 (2005).
[57] I. I. Sannikov, A. A. Ivanov, A. V. Kuznetsov, A. P. Menushenkov, and O. A. Churkin, Bull. of the Lebedev Phys. Inst. **41**, 215 (2014).
[58] I. I. Sannikov, A. A. Ivanov, A. V. Kuznetsov, A. P. Menushenkov, and O. A. Churkin, Physics Procedia **65**, 113 (2015).
[59] Only the copper tube temperature is controlled in our magnetometer. Overlapping tube inner cross section, large samples make convection of the heat-exchange gas more difficult. As a sequence sample's and tube's temperatures can differ if $T$ changes rapidly.
[60] At the critical current the Joule heat density is calculated as $W_c = E_c J_c$. The electric field is estimated as $E_c = \mathcal{A}\rho_{\rm FF} J_c/$ where $\rho_{\rm FF}(H,T)$ is the resistivity of the vortex motion and $\mathcal{A}$ is a constant of the order of unity.[3,4] Taking for magnetic field of 1 kOe $\rho_{\rm FF} \gtrsim 10-60$ n$\Omega$·cm (Refs. 85 and 86) and $J_c > 10^7 - 10^6$ A/cm$^2$ (Refs. 10, 12, 20, 23, and 26) in the range from the liquid helium to the liquid nitrogen temperatures we estimated $E_c \gtrsim (100-60)$ mV/cm and $W_c \gtrsim 1 - 0.06$ MW/cm$^3$.
[61] The transport current is determined as a rule using the electric field criterion 0.1–1 $\mu$V/cm. For induced currents the field depends on type of measurements. $E \simeq$ 0.01–0.1 $\mu$V/cm for vibrating sample magnetometry if $H$ is swept with the rate of 10–100 Oe/s.[26,87] $E \simeq$ 0.01–0.1 nV/cm for standard SQUID magnetometry. During relaxation measurements in the time window about 1 minute to 10 hours $E$ changes in the range 100–0.01 pV/cm.
[62] B. M. Lairson, J. Z. Sun, J. C. Bravman, and T. H. Geballe, Phys. Rev. B **42**, 1008 (1990).
[63] Explanation of $J(T)$ behavior based on Josephson coupling of nano-sized domains and presence of nano-sized inclusions of underdoped phase in $YBa_2Cu_3O_{7-\delta}$ films[31,32,88,89] is not discussed in this paper since it completely ignores pinning.
[64] F. C. Klaassen, G. Doornbos, J. M. Huijbregtse, R. C. F. van der Geest, B. Dam, and R. Griessen, Phys. Rev. B **64**, 184523 (2001).
[65] R. Griessen, W. Hai-hu, A. J. J. van Dalen, B. Dam, J. Rector, H. G. Schnack, S. Libbrecht, E. Osquiguil, and Y. Bruynseraede, Phys. Rev. Lett. **72**, 1910 (1994).
[66] Spatial variations in the critical temperature $T_c$ and in the charge carrier mean free path $\ell$ near lattice defects lead respectively to $\delta T_c$ and $\delta\ell$ pinning[3,65].
[67] L. F. Schneemeyer, E. M. Gyorgy, and J. V. Waszczak, Phys. Rev. B **36**, 8804 (1987).
[68] S. Senoussi, M. Oussena, G. Collin, and I. A. Campbell, Phys. Rev. B **37**, 9792 (1988).
[69] D. K. Christen and J. R. Thomson, Nature **366**, 98 (1993).
[70] B. Martínez, X. Obradors, A. Gou, V. Gomis, S. Piñol, J. Fontcuberta, and H. Van Tol, Phys. Rev. B **53**, 2797 (1996).
[71] J. Plain, T. Puig, F. Sandiumenge, X. Obradors, and J. Rabier, Phys. Rev. B **65**, 104526 (2002).
[72] J. Deak, M. McElfresh, J. R. Clem, Z. Hao, R. M. M. Konczykowski, S. Foltyn, and R. Dye, Phys. Rev. B **49**, 6270 (1994).
[73] A. Schilling, F. Hulliger, and H. Ott, Physica C **168**, 272 (1990).
[74] P. Zimmermann, H. Keller, S. L. Lee, I. M. Savić, M. Warden, D. Zech, R. Cubitt, E. M. Forgan, E. Kaldis, J. Karpinski, and C. Krüger, Phys. Rev. B **52**, 541 (1995).
[75] Z. Hao, J. R. Clem, M. W. McElfresh, L. Civale, A. P. Malozemoff, and F. Holtzberg, Phys. Rev. B **43**, 2844 (1991).
[76] J. D. Jorgensen, B. W. Veal, A. P. Paulikas, L. J. Nowicki, G. W. Crabtree, H. Claus, and W. K. Kwok, Phys. Rev. B **41**, 1863 (1990).
[77] S. Bosma, S. Weyeneth, R. Puzniak, A. Erb, A. Schilling, and H. Keller, Phys. Rev. B **84**, 024514 (2011).
[78] A. Barone, A. I. Larkin, and Y. N. Ovchinnikov, J. Supersond. **3**, 155 (1990).
[79] B. I. Ivlev and N. B. Kopnin, J. Low Temp. Phys. **80**, 161 (1990).
[80] D. Feinberg and C. Villard, Mod. Phys. Lett. B **4**, 9 (1990).
[81] D. Feinberg and C. Villard, Phys. Rev. Lett. **65**, 919 (1990).
[82] E. H. Brandt, Phys. Rev. B **58**, 6506 (1998).
[83] Eq. (15) is valid for applied fields $H <$ 10 kOe, at high fields the dependence $J_{cd}(T,B)$ is more complicated since a dislocation density becomes greater than the vortex density and some function is needed to accommodate vortices and dislocations[14,42].
[84] Expression similar to (17) was first obtained from OI theory in Ref. 19 but authors incorrectly approximated field dependence of the current as $J_{ci} \propto b^{-5/8}$.
[85] M. Golosovsky, M. Tsindlekht, H. Chayet, and D. Davidov, Phys. Rev. B **50**, 470 (1994).
[86] A. Maeda, H. Kitano, and R. Inoue, J. Phys.: Condens. Matter **17**, R143 (2005).
[87] I. A. Golovchanskiy, A. V. Pan, O. V. Shcherbakova, and S. A. Fedoseev, J. Appl. Phys. **114**, 164910 (2013).
[88] H. Darhmaoui and J. Jung, Phys. Rev. B **53**, 14621 (1996).
[89] H. Darhmaoui and J. Jung, Phys. Rev. B **57**, 8009 (1998).